Molecular Biology of the Cell
Vol. 21, 2732–2745, August 1, 2010

Autosomal Recessive Polycystic Kidney Disease Epithelial Cell Model Reveals Multiple Basolateral Epidermal Growth Factor Receptor Sorting Pathways

Sean Ryan,* Susamma Verghese,† Nicholas L. Cianciola,* Calvin U. Cotton,†‡ and Cathleen R. Carlin*†§

Departments of *Molecular Biology and Microbiology, †Physiology and Biophysics, ‡Pediatrics, and §Case Western Reserve University Comprehensive Cancer Center, School of Medicine, Case Western Reserve University, Cleveland, OH 44106-4970

Submitted December 22, 2009; Accepted May 26, 2010
Monitoring Editor: Keith E. Mostov

Sorting and maintenance of the EGF receptor on the basolateral surface of renal epithelial cells is perturbed in polycystic kidney disease and apical expression of receptors contributes to severity of disease. The goal of these studies was to understand the molecular basis for EGF receptor missorting using a well-established mouse model for the autosomal recessive form of the disease. We have discovered that multiple basolateral pathways mediate EGF receptor sorting in renal epithelial cells. The polycystic kidney disease allele in this model, Bicc1, interferes with one specific EGF receptor pathway without affecting overall cell polarity. Furthermore one of the pathways is regulated by a latent basolateral sorting signal that restores EGF receptor polarity in cystic renal epithelial cells via passage through a Rab11-positive subapical compartment. These studies give new insights to possible therapies to reconstitute EGF receptor polarity and function in order to curb disease progression. They also indicate for the first time that the Bicc1 gene that is defective in the mouse model used in these studies regulates cargo-specific protein sorting mediated by the epithelial cell specific clathrin adaptor AP-1B.

INTRODUCTION

The nephron is the basic structural and functional unit of the kidney (Kriz and Kaissing, 2008). Each nephron has an initial filtering component composed of a glomerulus and Bowman's capsule connected to a long convoluted tubule lined by transporting epithelia. Epithelial cell polarity is vitally important for correct function of different tubule segments (Kriz and Kaissing, 2008). In addition to the apicobasolateral axis, most renal epithelial cells exhibit planar polarity featuring primary cilia extending from the apical membrane (Fischer and Pontoglio, 2009). Cell polarity defects have been linked to a number of hereditary kidney diseases including polycystic kidney diseases (PKDs) characterized by the accumulation of fluid-filled cysts in the cortex and medulla (Igarashi and Somlo, 2002; Grantham, 2003; Harris and Torres, 2009). Approximately 50% of afflicted individuals develop end-stage renal disease requiring dialysis or kidney transplantation before the age of 60. Although presently incurable, improved understanding of disease mechanisms is uncovering new prospects for effective pathophysiology-based therapies (Torres and Harris, 2006). Cystic cells and tissues are also unique cell biological models for studying polarized sorting mechanisms.

Human PKD susceptibility genes encode large membrane proteins. PKD1 and PKD2 are involved in the autosomal dominant form of the disease (ADPKD), and fibrocystin is defective in autosomal recessive PKD (ARPKD; International Consortium for Polycystic Kidney Disease, 1995; The American Consortium for PKD1, 1995; Mochizuki *et al.*, 1996; Onuchic *et al.*, 2002; Ward *et al.*, 2002). Multiple lines of evidence indicate these proteins are functionally related, and all three localize to primary cilia, suggesting these organelles have a critical role in cyst formation (Yoder, 2007; Zhou, 2009). Model organisms have also advanced our current understanding of PKD pathophysiology (Guay-Woodford, 2003; Wilson and Robert, 2008). Some models involve targeted disruptions in PKD orthologues or genes that regulate ciliogenesis. Others such as the BPK (deficient in B-cell progenitor kinase) model arose by spontaneous mutations leading to identification of novel PKD susceptibility genes. The BPK disease susceptibility allele encodes Bicc-1, an mRNA-binding protein involved in posttranscriptional polyadenylation and mRNA stability (Cogswell *et al.*, 2003; Chicoine *et al.*, 2007). The BPK mouse has the same broad spectrum of renal and hepatic involvement as ARPKD and played a major role in furthering our understanding of the human disease before fibrocystin was discovered (Nauta *et al.*, 1993; Sweeney and Avner, 2006). The BPK mouse also provides

This article was published online ahead of print in *MBoC in Press* (http://www.molbiolcell.org/cgi/doi/10.1091/mbc.E09–12–1059) on June 2, 2010.

Address correspondence to: Cathleen Carlin (cathleen.carlin@case.edu).

Abbreviations used: AD, autosomal dominant; AP, adaptor protein complex; AR, autosomal recessive; ARE, apical recycling endosome; ASE, apical sorting endosome; BPK, deficient in B-cell progenitor kinase; BSE, basolateral sorting endosome; CRE, common recycling endosome; EGFR, EGF receptor; ER, endoplasmic reticulum; PKC, protein kinase C; PKD, polycystic kidney disease; PMA, phorbol 12-myristate 13-acetate; TfR, transferrin receptor; TGN, *trans*-Golgi network.

novel insights to cyst formation during prenatal development and is an important model for evaluating new PKD therapies (Sweeney *et al.*, 2000, 2008; Sweeney and Avner, 2006).

ErbB receptor tyrosine kinases (EGF receptor or EGFR, ErbB2, ErbB3, and ErbB4) and their respective ligands have important roles in kidney development and tubule repair (Zeng *et al.*, 2009). EGFR is normally sorted to basolateral membranes in adult tubular epithelial cells (Goodyer *et al.*, 1988; Sack and Talor, 1988). However, numerous primary PKD genetic defects perturb EGFR polarity, leading to increased apical expression (Sweeney *et al.*, 2000). EGF and EGF-like ligands are also secreted into the apical medium of cultured cystic epithelial cells and are detected in cyst fluid from ADPKD patients (Wilson, 2004). Importantly, EGFR tyrosine kinase inhibition significantly improves kidney function and reduces morbidity in PKD animal models (Richards *et al.*, 1998; Sweeney *et al.*, 2000; Torres *et al.*, 2003). These observations suggest chronic EGF signaling from the apical membrane is a common disease progression factor in multiple forms of PKD.

Polarized sorting is mediated by highly specialized subcellular machinery that recognizes specific sorting signals in membrane protein cargo (Nelson and Rodriguez-Boulan, 2004; Rodriguez-Boulan *et al.*, 2005; Bryant and Mostov, 2008; Mellman and Nelson, 2008; Heike *et al.*, 2009). These interactions target newly synthesized molecules from the *trans*-Golgi network (TGN) to the plasma membrane, recycle internalized cargo back to the same plasma membrane domain, and facilitate transcytosis from one pole of the cell to the other. Apical sorting is regulated by diverse signals including glycosylphosphatidylinositol (GPI) anchors that partition into lipid rafts and N-glycans that are sorted by unknown mechanisms. Although both pathways have the same final destination, lipid-raft– and *N*-glycan–dependent cargoes traverse different endosome intermediates called apical sorting endosomes (ASEs) and apical recycling endosomes (AREs), respectively (Cresawn *et al.*, 2007; Weisz and Rodriguez-Boulan, 2009). Basolateral sorting is usually regulated by short linear amino acid signals located in the cytosolic tails of protein cargoes (Rodriguez-Boulan *et al.*, 2005; Bryant and Mostov, 2008; Mellman and Nelson, 2008; Heike *et al.*, 2009). The epithelial cell–specific clathrin adaptor protein complex AP-1B recognizes some of these signals in common recycling endosomes (CREs; Fölsch *et al.*, 1999; Ohno *et al.*, 1999; Gan *et al.*, 2002). Relatively less is known about AP-1B–independent pathways that may target the basolateral membrane directly or via basolateral sorting endosome (BSE) intermediates (Heike *et al.*, 2009). Polarized sorting is also regulated by the multiprotein exocyst complex involved in tethering, docking, and fusion of post-Golgi transport vesicles with the plasma membrane (Wu *et al.*, 2008). In addition to the core machinery, some cargoes require additional specialized exocyst components (Wu *et al.*, 2008).

Our data provide new molecular insights into how EGFR membrane polarity is regulated by multiple hierarchical sorting pathways in renal epithelial cells. Not all the pathways are perturbed in the BPK mouse, which has important implications for understanding PKD pathogenesis and designing novel therapeutic approaches. Furthermore EGFR sorting plasticity may explain why PKD perturbs trafficking of specific membrane cargo without disrupting renal epithelial cell barrier function.

MATERIALS AND METHODS

Antibodies and Reagents

The following antibodies were purchased: actin, AP-1 γ-subunit, AP-2 α-subunit, and ezrin mouse monoclonal antibodies (mAb) from Sigma (St. Louis, MO); β-catenin, CD73, E-cadherin, and pan-Erk mouse monoclonal antibodies from BD Biosciences (San Diego, CA); CD73 and c-MET rabbit polyclonal antibodies from Santa Cruz Biotechnology (Santa Cruz, CA); EGFR rabbit polyclonal antibody from Research Diagnostic (Flanders, NJ); mouse-specific EGFR goat polyclonal antibody from R&D Systems (Minneapolis, MN); phospho-specific EGFR (Thr654) mouse mAb from Abcam (Cambridge, MA); phospho-specific mitogen-activated protein kinase (MAPK) rabbit and biotin HRP-conjugated goat polyclonal antibodies from Cell Signaling (Beverly MA); Rab11 rabbit polyclonal antibody and transferrin mouse mAb from Zymed (San Francisco, CA); and transferrin receptor mouse mAb from Leinco (Ballwin, MO). ZO-1 rat mAb was obtained from Developmental Studies Hybridoma Bank developed under the auspices of NICHD and maintained by The University of Iowa Department of Biological Sciences (Iowa City, IA). Human-specific EGFR1 mouse mAb was produced using the ascites method (Harlow and Lane, 1988). Detyrosinated tubulin ID5 mouse mAb was a gift from J. Wehland (Gesellschaft für Biotechnologische Forschung, Braunschweig, Germany). A previously published AP-1B μ1B-subunit specific antibody (Fölsch *et al.*, 1999) was a gift from I. Mellman (Yale University, New Haven, CT). Rabbits were immunized with synthetic peptides corresponding to sequences from mouse Bicc-1 (NCBI Reference Sequence NM_031397) and human fibrocystin (NCBI Reference Sequence NP_619639). Conjugated secondary antibodies were purchased from Jackson ImmunoResearch Laboratories (Fort Washington, PA), biotin and streptavidin reagents from Pierce (Rockland, IL), and receptor-grade mouse EGF and phorbol 12-myristate 13-acetate (PMA) from Sigma.

Cloning and Mutagenesis

Nucleic acids coding for human EGFR juxtamembrane residues 652–697 were PCR-amplified from a full-length EGFR/pCB6$^+$ template described in (Hobert and Carlin, 1995). The following primers replaced the alanine residue at position 698 with a stop codon (bold) and incorporated novel BamHI (underlined) and EcoRV sites (italics): Forward: 5′-GTAATCGGATCCAAAAGAGAACACTGCGGAGGCTG; Reverse: 5′-ATC*GATATC***TTA**ACCGGAGCCCAGCACTTTG-3′.

Gel-purified PCR product was digested with BamHI and Eco RV, and ligated to BamHI and SmaI sites in pGEX-3X to produce a glutathione *S*-transferase (GST) fusion protein in *Escherichia coli* (Amersham-Pharmacia, Piscataway, NJ). Nucleic acids coding for the dileucine motif at positions 658 and 659 were mutagenized to a di-alanine and threonine residue 654 to alanine or aspartic acid, using the EGFR-Jx/pGEX-3X template, a Quick Change Mutagenesis kit (Invitrogen, Carlsbad, CA), and the following primers (mutations in bold): 658-AA: forward, 5′-AGAACACTGCGGAGG**GCG-GCG**CAGGAGAGGGAGCTT-3′ and reverse, 5′-AAGCTCCCTCTCCTG**CG-CCG**CCCTCCGCAGTGTTCT-3′; T654A: forward, 5′-CGTGGGATCCAA-AAGA**GCA**CTGCGGAGGCTGCTGCAG-3′ and reverse, 5′-CTGCAGCAGC-CTCCGCAG**TGC**TCTCTTTTGGATCCCACG-3′; and T654D: forward, 5′-CGTGGGATCCAAAAGA**GAT**CTGCGGAGGCTGCTGCAG-3′ and reverse, 5′-CTGCAGCAGCCTCCGCAG**ATC**TCTCTTTTGGATCCCACG-3′.

The 658-AA and T654D substitutions were also introduced to full-length human EGFR cloned in the eukaryotic expression plasmid pBKΔlac^p-CMV (Kil *et al.*, 1999) and these mutagenic primers (mutations in bold): 658-AA: forward, 5′-AGCGCACGCTGCGGAGG**GCTGCT**CAGGAGAGGGAGCTT-GTGGAG-3′ and reverse, 5′-CTCCACAAGCTCCCTCTCCTG**AGCAGC**C-CTCCGCAGCGTGCGCT-3′; and T654D: forward, 5′-ACATCGTTCGGAAG-CGC**GAT**CTGCGGAGGCTGCTGCA-3′ and reverse, 5′-TGCAGCAGC-CTCCGCAG**ATC**GCGCTTCCGAACGATGT-3′.

Wild-type and mutant EGFR constructs were then subcloned into the pQCXIN bicistronic retroviral packaging vector (BD Biosciences) using the NotI restriction sites upstream of the IRES (internal ribosome entry site) element and neomycin resistance gene.

PCR primers were designed using the DNASTAR software package (DNASTAR, Madison, WI), and all PCR products were sequenced in their entirety by automated DNA sequencing.

Renal Epithelial Cell Culture Models

The conditionally immortalized cell lines used in this study were isolated from normal and cystic animals bred with an H-2k^b-*ts*A58 transgenic strain expressing temperature-sensitive SV40 T-antigen under the control of a γ-interferon (γ-IFN) inducible promoter (Sweeney *et al.*, 2001). These cells were propagated in serum-free defined medium consisting of a 1:1 mixture of Dulbecco's-modified Eagle's medium and Ham's F-12 medium, supplemented with insulin (8.3×10^{-7} M), prostaglandin E_1 (7.1×10^{-8} M), selenium (6.8×10^{-9} M), transferrin (6.2×10^{-8} M), triiodothyronine (2×10^{-9} M), dexamethasone (5.09×10^{-8} M), and recombinant γ-IFN (10 U/ml; GIBCO-BRL, Gaithersburg, MD) at permissive temperature (33°C). Confluent cultures were refed daily with γ-IFN–free medium supplemented with 5% fetal bovine serum (FBS) for 4–6 d at nonpermissive temperature (37°C) to

facilitate terminal differentiation. Madin-Darby canine kidney (MDCK) and pig LLCPK1 renal epithelial cell models were maintained in minimal essential medium (MEM) or MEM-α, respectively, supplemented with 10% FBS and 2 mM glutamine. All renal cell lines were seeded on polycarbonate Transwell filter inserts (0.4-μm pore size; Costar, Cambridge, MA) at high density to generate electrically resistant monolayers suitable for domain-specific assays ~4 d later.

Quantitative PCR

RNA was extracted using a ToTALLY RNA kit (Applied Biosystems, Foster City, CA) and reverse-transcribed with the SuperScript First-Strand Synthesis System (Invitrogen). Target gene mRNA levels were analyzed by quantitative PCR (qPCR) using standard hydrolysis probe (TaqMan; Applied Biosystems) techniques and a glyceraldehyde 3-phosphate dehydrogenase (GAPDH) internal control. The following primer pairs were designed using the Roche Universal Probe Library Assay Design Center (Indianapolis, IN; mouse μ1B) or Primer3 software (http://www.simgene.com/Primer3; GAPDH): μ1B: forward, 5′-ACCGAGTGCTCTTTGAGCTT-3′ and reverse, 5′-CACATCTTCCAGTTCCACAGAC-3′; and GAPDH: forward, 5′-ATGGGAAGCTGGTCATCAAC-3′ and reverse, 5′-GTGGTTCACACCCATCACAA-3′.

Probes and PCR master mix were purchased from Roche, and primers from Operon (Huntsville, AL). PCR was performed on a model 7500 real-time PCR system, and products were analyzed using 7500 System SDS software version 1.3 (Applied Biosystems). The mRNA expression levels for cystic cells were plotted as fold change relative to mRNA levels from normal mouse collecting duct cells.

Retroviral Gene Transfer

Recombinant retroviruses expressing wild-type and mutant human EGFRs were produced in HEK (human embryonic kidney) GP2–293 packaging cells using established methods. Cell populations with stable human EGFR expression were generated by selection in 200 μg/ml G418 (Calbiochem, San Diego, CA) for 10–14 d followed by 2–3 rounds of human EGFR enrichment using sterile flow cytometry after cells were stained with EGFR1 antibody (Hobert *et al.,* 1997).

Microscopy

For scanning electron microscopy filter-grown cells were fixed with 2.5% glutaraldehyde in 0.1 M cacodylate buffer, pH 7.4, postfixed in 2% osmium tetroxide, dehydrated in graded ethanol, and subjected to critical point drying in liquid CO_2. Excised filters were mounted on aluminum stubs, sputter-coated with platinum, and viewed on a JEOL JSM-840 scanning electron microscope (Peabody, MA) at ×3000 magnification. For confocal microscopy, samples were prepared using a published method (Crooks *et al.,* 2000). Briefly, cells were perforated with 0.5% β-escin in a solution of 80 mM PIPES, pH 6.8, supplemented with 5 mM EGTA and 1 mM $MgCl_2$ for 5 min and fixed with 3% paraformaldehyde-phosphate-buffered saline (PBS) for 15 min. Cells were stained with primary or secondary antibodies overnight at 4°C or for 1 h at room temperature. Antibodies were diluted in a solution containing 0.5% β-escin and 3% radioimmunoassay-grade bovine serum albumin (BSA) and samples were blocked with a solution containing 1% normal serum from the host animal used to generate the secondary antibody between incubations with primary and secondary antibodies. Alternatively cells were fixed with 3% paraformaldehyde-PBS for 15 min and incubated with antibodies added to apical or basolateral surfaces to detect extracellular epitopes (Hobert *et al.,* 1997). Cells were optically sectioned with a Zeiss LSM 510 Meta laser scanning microscope equipped with argon and helium-neon lasers (Carl Zeiss MicroImaging, Jenna, Germany). Image resolution with a Zeiss 100× Plan Apo, NA 1.4 oil immersion objective and Zeiss LSM software was 1024 × 1024 pixels.

Domain-specific Biotinylation and Triton X-100 Extractability

Filter-grown cells were rinsed three times with PBS supplemented with 1 mM $CaCl_2$ and 1 mM $MgCl_2$ (PBS-CM) and then incubated for 30 min at 4°C with EZ-Link Sulfo-NHS-LC-biotin (1 mg/ml) dissolved in borate buffer (85 mM NaCl, 4 mM KCl, 15 mM $Na_2B_4O_7$, pH 9.0) or PBS-CM added to the apical or basolateral surface, respectively. The reaction was quenched with 50 mM NH_4Cl, and cells were lysed with a solution of 1% (wt/vol) Triton X-100 (TX-100) in 20 mM Tris, pH 8.0, 50 mM NaCl, 5 mM EDTA, 0.2% BSA, 0.2 mM phenylmethylsulfonyl fluoride, and 1 mM leupeptin (immunoprecipitation buffer). Experiments to determine temperature sensitive TX-100 extractability were carried out as described in (Brown and Rose, 1992). Briefly, cells were lysed with 0.5% (vol/vol) TX-100 in 10 mM Tris, pH 7.5, supplemented with 120 mM NaCl, 25 mM KCl, 2 mM EDTA, 2 mM EGTA, 0.2 mM phenylmethylsulfonyl fluoride, and 1 mM leupeptin. Lysates were incubated on ice or at 37°C for 30 min and clarified by high-speed centrifugation.

Pulse-Chase Experiments

Filter-grown cells were preincubated in methionine- and cysteine-free medium for 1 h. The amino acid–starved cells were pulse-labeled from the basolateral surface with ^{35}S-Express Protein Labeling Mix (2.5 mCi/ml; PerkinElmer Life Sciences, Boston, MA) diluted in amino acid–deficient medium supplemented with 10% dialyzed FBS and 0.2% BSA. The radio-labeled cells were then incubated at 37°C in medium supplemented with a 10-fold excess of nonradioactive methionine and cysteine (chase medium) for up to 3 h. In some experiments cells were preincubated for 2 h at 18°C followed by a 37°C recovery period. Cells were solubilized with immunoprecipitation buffer.

In Vitro Pulldown Assays

A synthetic peptide corresponding to human EGFR residues 645–677 (peptide 1) was coupled to Sepharose beads using an NHS-activated bead kit (Pierce). GST fusion proteins were purified from BL21 cells transformed with pGEX-3X plasmids encoding wild-type (peptide 2) and mutant (labeled 658-AA, T654A, and T654D in Figure 4B) EGFR juxtamembrane sequences. Bacteria were cultured at 37°C until reaching OD_{600}, induced with 0.1 mM IPTG (isopropyl-ß-D-thiogalactopyranoside) for 16 h at room temperature, and collected by low-speed centrifugation. Cells were subjected to one freeze-thaw cycle and lysed with B-PER solution according to the manufacturer's instructions (Pierce). Supernatants were adjusted to 3% TX-100 and incubated with glutathione-Sepharose beads (Amersham-Pharmacia) for 20 min at 4°C with rotation. Beads with attached fusion proteins were incubated with crude subcellular fractions enriched for clathrin adaptors according to published methods (Robinson, 1993; Cianciola *et al.,* 2007). Briefly, cells were scraped in PBS supplemented with 2 mM EDTA, 5 mM EGTA, and protease inhibitors, resuspended in 0.1 M MES, pH 6.5, 0.2 M EDTA, 0.5 mM $MgCl_2$, 0.02% NaN_3, 10 mg/ml BSA, and protease inhibitors, and lysed with 1% NP-40 for 5 min at room temperature. Postnuclear supernatants were centrifuged at 60,000 × *g* for 30 min to collect a crude cytosol fraction. Membrane pellets were resuspended in the NP-40 lysis buffer and incubated with 0.5 M Na_2CO_3 for 5 min on ice to release peripheral membrane proteins. Beads were incubated with peripheral membrane proteins for 1 h at room temperature followed by extensive washing, and bound proteins were eluted with Laemmli sample buffer and resolved by SDS-PAGE.

Immunoprecipitation and Immunoblotting

Immunoprecipitations were carried out using antibodies adsorbed to protein A-Sepharose CL-4B beads (Sigma). Immune complexes containing biotinylated proteins were boiled for 5 min in 100 μl of 10% SDS, and SDS-protein solutions were diluted with immunoprecipitation buffer and incubated with streptavidin-agarose beads for 16 h at 4°C. Affinity-purified protein complexes were eluted with Laemmli sample buffer and resolved by SDS-PAGE. Gels with radioactive proteins were treated with En^{3}Hance (PerkinElmer-NEN, Wilmington, DE) for fluorography. Nonradioactive affinity-purified protein complexes or equal aliquots of total cellular protein were resolved by SDS-PAGE and transferred to nitrocellulose membranes using standard methods. Nitrocellulose filters were incubated with primary antibodies followed by isoform-specific HRP-conjugated secondary antibodies for detection by enhanced chemiluminescence (Amersham-Pharmacia).

Image Preparation

Digital images were prepared using Adobe Photoshop CS4 and Adobe Illustrator CS4 software packages (San Jose, CA).

RESULTS

Cell Culture Models Derived from the BPK Mouse

Although the BPK model has been studied for nearly two decades (Nauta *et al.,* 1993), the underlying *Bicc1* gene defect was only recently identified (Cogswell *et al.,* 2003). The goal of these experiments was to characterize *Bicc1* gene products in conditionally immortalized cell lines from cystic animals and normal age-matched controls. Endogenous protein expression was analyzed with a newly developed antibody to the Bicc1 amino terminus. The *Bicc1* gene has 22 exons encoding two splice variants in mouse kidney (Figure 1A). Exon 21 is spliced out of transcript A and transcript B encompasses the entire open reading frame (Cogswell *et al.,* 2003). However, a two-nucleotide frame-shift in the mutant allele produces an abnormal transcript A in cystic animals. Furthermore, a premature stop codon in exon 21 truncates transcript B. The Bicc1 antibody detected one major protein species from normal renal cells, in contrast to cystic cells that

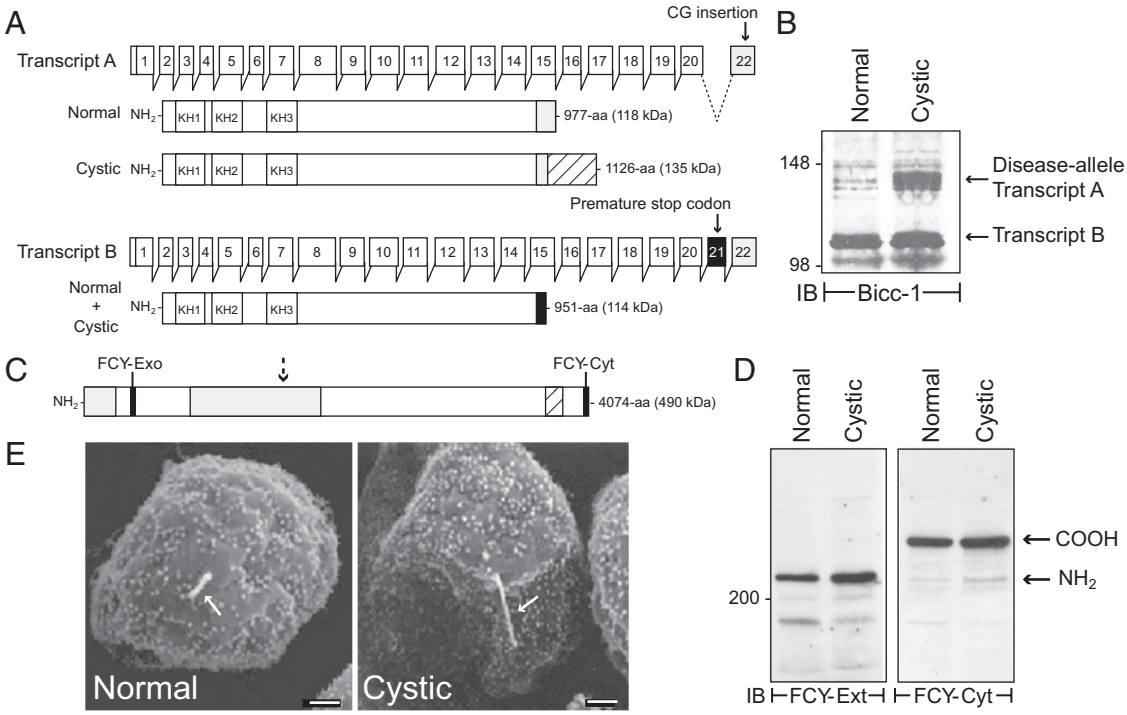

Figure 1. Conditionally immortalized cell lines from ARPKD mouse model. (A) The *Bicc1* gene has 22 exons encoding two alternatively spliced transcripts (A and B) in mouse kidney. Predicted structures for normal and disease-specific protein products shown beneath each transcript highlight RNA-binding KH (K homology) domains, exon 21 and exon 22-encoded sequences (black and gray boxes, respectively), disease-specific carboxyl-terminal extension (hatched box), and predicted molecular weights (in parenthesis). Adapted from Cogswell *et al.* (2003). (B) Equal protein aliquots were immunoblotted with Bicc1 antibody. (C) Predicted fibrocystin domain structure highlighting extracellular immunoglobulin-like TIG repeats (light gray box), transmembrane domain (hatched box), FCY-Exo and FCY-Cyt peptide antibody sequences (black box), and approximate cleavage site generating major endogenous protein species (dashed arrow). (D) Equal protein aliquots were immunoblotted with fibrocystin antibodies (FCY-Ext and FCY-Cyt described in text). (E) Cells were examined by scanning electron microscopy. Arrow, central primary cilia. Scale bar, 1 μm; magnification, $\times$3000.

exhibited an additional higher molecular protein consistent with the presumptive size of disease-specific transcript A (Figure 1B). Because the cystic cells were derived from a *Bicc1* $-/-$ homozygous animal (Sweeney *et al.*, 2001), the protein species detected in both cell lines probably corresponds to the presumptive product of transcript B (Figure 1A). We also determined whether the disease allele impairs molecules or organelles linked to other primary ARPKD genetic defects. The predicted structure for fibrocystin is shown in Figure 1C (Harris and Torres, 2009). In contrast to recombinant fibrocystin that is posttranslationally processed into multiple peptide fragments (Hiesberger *et al.*, 2006; Kaimori *et al.*, 2007), the bulk of the endogenous mouse protein is cleaved once in both cell lines (Figure 1D). Based on size and reactivity with two newly developed fibrocystin antibodies, the endogenous protein is apparently digested at an extracellular domain site previously identified in the recombinant protein (Figure 1, C and D; Hiesberger *et al.*, 2006). The Oak Ridge Polycystic Kidney (ORPK) mouse model of ARPKD involves an intraflagellar transport protein necessary for ciliogenesis (Yoder *et al.*, 2002). The ORPK defect causes loss or severe stunting of primary cilia (Brown and Murcia, 2003). In contrast, conditionally immortalized cell lines from the BPK model had morphologically similar primary cilia (Figure 1E) ranging in length from 1 to 2.5 μm according to (Veizis *et al.*, 2004). Altogether these data provide the first experimental evidence that Bicc1 proteins are produced in the BPK model. The cystic cells translate both transcripts in contrast to normal cells that express transcript B. Furthermore the disease allele does not perturb fibrocystin expression or ciliogenesis.

Normal and Cystic Cells Exhibit Similar Distributions of Multiple Epithelial Cell Polarity Markers

The goal of these experiments was to determine whether conditionally immortalized normal cells exhibit properties of renal epithelial cells and if the disease allele perturbs overall cell polarity. Cells were stained with antibodies to a number of epithelial cell markers, and Figure 2A shows vertical optical sections exhibiting polarized expression for each molecule. Primary cilia were identified with antibodies to detyrosinated tubulin and fibrocystin that are both typically associated with this organelle (Jensen *et al.*, 1987; Ward *et al.*, 2003). These images confirm data in Figure 1E indicating cystic cells have primary cilia and also demonstrate that the disease allele does not impair fibrocystin localization. Normal and cystic cells both displayed GPI-anchored CD73 on apical membranes (Figure 2A; Strohmeier *et al.*, 1997). The punctate CD73 staining pattern is typical for proteins enriched in microvilli on the apical surface (Strohmeier *et al.*, 1997). Both cell lines also exhibited ZO-1–positive tight junctions at the apex of the lateral membrane and β-catenin on lateral cell membranes (Figure 2A; Stevenson *et al.*, 1986; Nelson, 2008). Importantly, the transferrin receptor (TfR) that requires AP-1B for polarized membrane expression was localized to lateral membranes in both cell lines (Fölsch *et al.*, 1999; Figure 2A). Using qPCR, we demonstrated that normal and cystic cells both express the epithelial specific clathrin

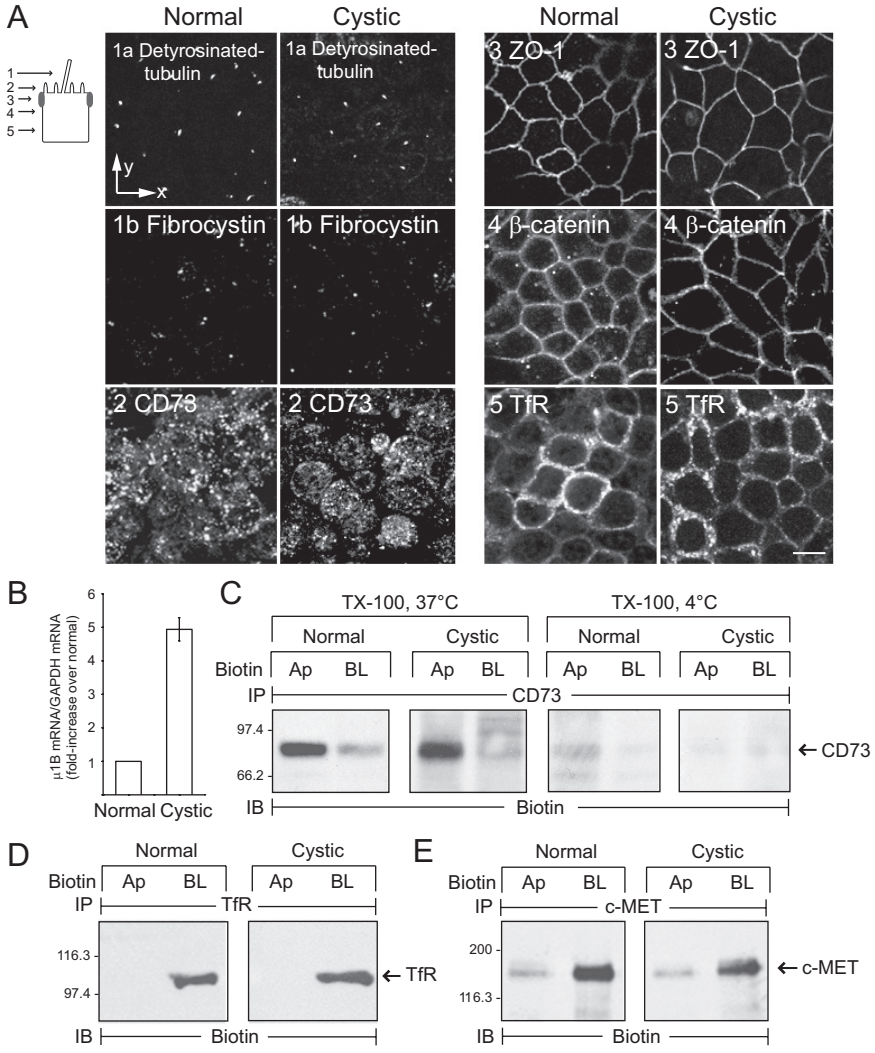

Figure 2. Epithelial cell markers expressed normally in conditionally immortalized cell lines. (A) Selected vertical x-y confocal optical sections (see schematic) from permeabilized cells stained with antibodies listed in figure. Scale bar, 5 μm. (B) AP-1B μ1B subunit mRNA was measured by qPCR and normalized to an internal GAPDH control. Results for cystic cells (mean ± SEM, n = 4) are presented as fold increase relative to μ1B mRNA expression in normal cells, which was set to 1. (C) Cells were harvested with TX-100 buffer at 37 or 4°C after domain-specific biotinylation. (D and E) Biotinylated cells were harvested with immunoprecipitation buffer at 4°C. (C–E) Cargo-specific immune complexes were immunoblotted for biotin. Ap, apical; BL, basolateral.

adaptor AP-1B μ1B subunit (Figure 2B). Interestingly the cystic cells express a 4–5-fold increase in μ1B subunit mRNA (Figure 2B) compared with normal renal cells. The domain-specific distribution for several proteins was also determined by analyzing immune complexes from filter-grown cells biotinylated at apical or basolateral surfaces. CD73 was localized to apical membranes and also soluble in TX-100 at 37 but not 4°C (Figure 2C), consistent with involvement of lipid raft carriers in CD73 trafficking (Brown *et al.*, 1989; Lisanti *et al.*, 1990). In addition to TfR (Figure 2D), biochemical data show that the receptor tyrosine kinase c-MET localizes to basolateral membranes in normal and cystic cells (Figure 2E; Crepaldi *et al.*, 1994). Altogether these data indicate both of the conditionally immortalized cell lines have expected distributions of typical epithelial cell polarity markers, have functional lipid raft– and AP-1B–dependent sorting machinery, and retain other receptor tyrosine kinases on the basolateral membrane.

EGFR Expression in Conditionally Immortalized Cell Lines

EGFR expression was analyzed using multiple experimental approaches. First, cells were stained with an antibody to endogenous mouse EGFR demonstrating basolateral expression in normal cells but nonpolar membrane distribution in cystic cells (Figure 3A). In contrast, both cell lines exhibited typical polarized distribution of the microfilament membrane linking protein ezrin just beneath the cell apex, as well as E-cadherin along lateral membranes (Figure 3A). Recombinant human EGFR also exhibited the same loss of membrane polarity in cystic cells as the endogenous receptor indicating the EGFR phenotype is an innate property of the cell and not the result of an unrecognized mutation in the endogenous receptor (Figure 3A). Second, ERK1/ERK2 (extracellular signal–regulated kinase 1/2) activity was monitored to assess domain-specific EGFR activation. Results indicate this pathway is induced by basolateral EGF in normal cells, but from both membranes in cystic cells (Figure 3B). Interestingly ERK1/ERK2 activation was significantly prolonged in basolaterally stimulated cystic cells compared with normal cells (Figure 3B), suggesting the disease allele perturbs EGFR cell signaling at both membrane domains. Third, newly synthesized receptors undergo similar molecular weight mobility shifts consistent with *N*-glycan maturation in normal and cystic cells (Figure 3C; Carlin and Knowles, 1986). Furthermore both cell lines have equivalent levels of total EGFR protein (Figure 3D). Taken together these results rule out incomplete glycosylation or insufficient basolateral sorting capacity as likely explanations for the cystic EGFR phenotype (Hobert *et al.*, 1999; Tan *et al.*, 2003;

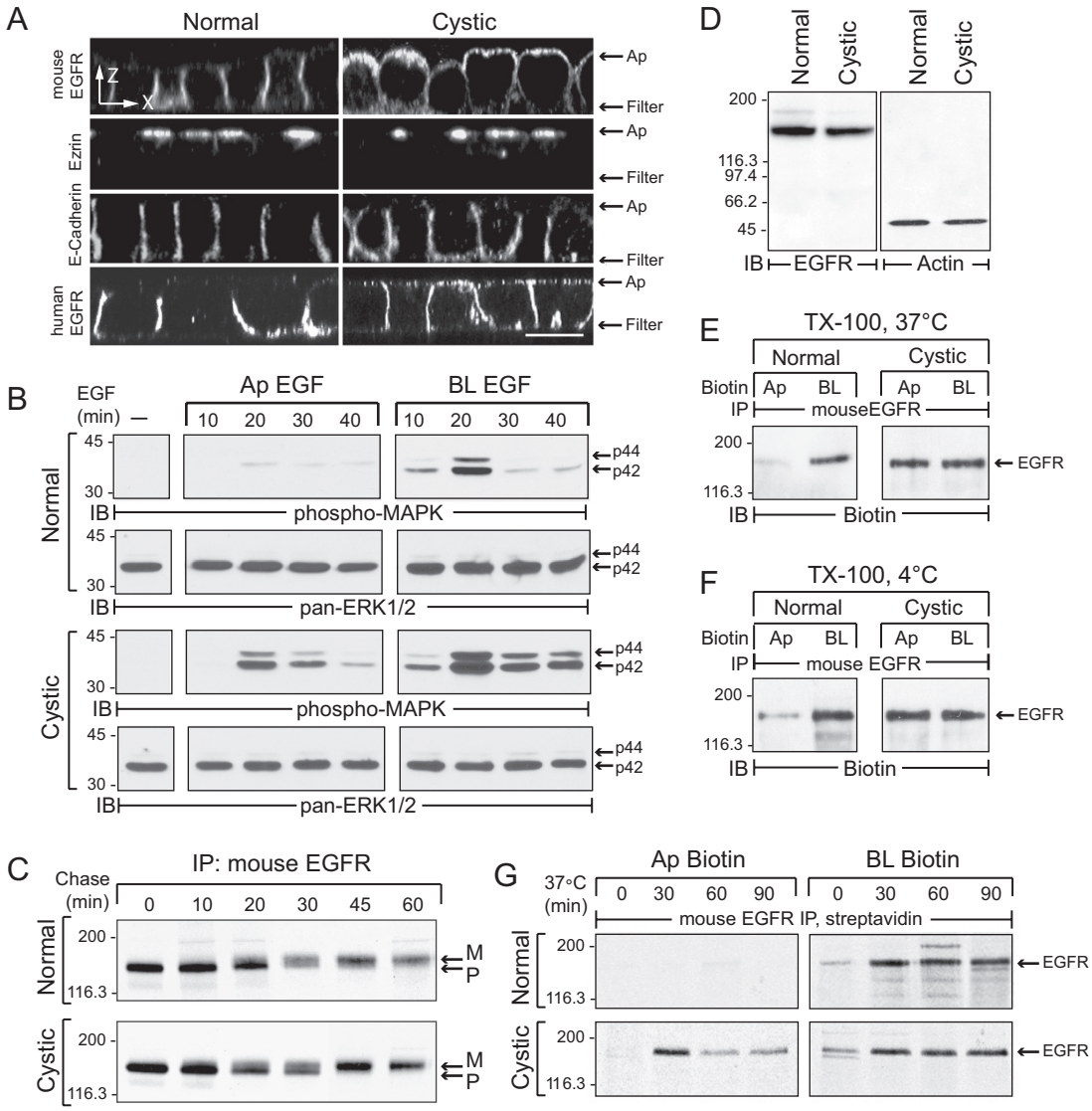

Figure 3. EGFR expression in conditionally immortalized cell lines. (A) Horizontal x-z optical sections of permeabilized cells stained with antibodies to proteins listed in the figure. Cells in bottom panels were transduced with a recombinant human EGFR retrovirus. Scale bar, 5 μm. (B) Cells were stimulated with domain-specific EGF (50 ng/ml) for times indicated. Equal protein aliquots were immunoblotted with activation-specific phospho-MAPK antibody followed by pan-ERK1/2 antibody to check protein loading. (C) Cells were pulse-labeled with ^{35}S-labeled amino acids and switched to chase medium for various times. Radiolabeled EGFR immune complexes were detected by fluorography after SDS-PAGE. P, precursor EGFR; M, mature EGFR. (D) Equal protein aliquots were immunoblotted for endogenous EGFR or β-actin. (E and F) Biotinylated cells were harvested with TX-100 buffer at 37°C (E) or 4°C (F), and mouse EGFR immune complexes were immunoblotted for biotin. (G) Pulse-labeled cells incubated in chase medium at 18°C for 2 h were biotinylated immediately or after a 37°C recovery period. Streptavidin affinity-purified mouse EGFR immune complexes were detected by fluorography.

Prydz *et al.*, 2007). Fourth, EGFRs were soluble with TX-100 at different temperatures (Figure 3, E and F), suggesting apical EGFR missorting involves a lipid raft–independent mechanism (Cresawn *et al.*, 2007). Finally, we examined domain-specific delivery of newly synthesized EGFR. These studies were carried out by synchronizing pulse-labeled proteins in the Golgi with an 18°C temperature block, followed by a 37°C recovery period to induce vesicle transport (Hunziker *et al.*, 1990). Results in Figure 3G indicate the bulk of newly synthesized EGFRs were biotin-accessible at apical and basolateral surfaces within the first 30 min of the 37°C recovery period in cystic cells. Apical delivery was completely blocked at 18°C in cystic cells. In contrast, basolateral delivery was reduced but not eliminated in either cell line, consistent with reported differences in temperature sensitivity for polarized sorting pathways (Hunziker *et al.*, 1990). The cystic cells also exhibited a modest reduction in radiolabeled apical EGFRs during the 37°C recovery period that is probably due to rapid equilibration of newly delivered apical molecules with biotin-inaccessible internal pools (Cresawn *et al.*, 2007).

LLCPK1 Cells Also Exhibit EGFR Sorting Abnormalities

Although both conditionally immortalized cell lines express functional AP-1B complexes, it is currently unclear whether this pathway contributes to polarized EGFR expression. This question was addressed in LLCPK1 cells that lack the endogenous AP-1B μ1B subunit resulting in defective sorting

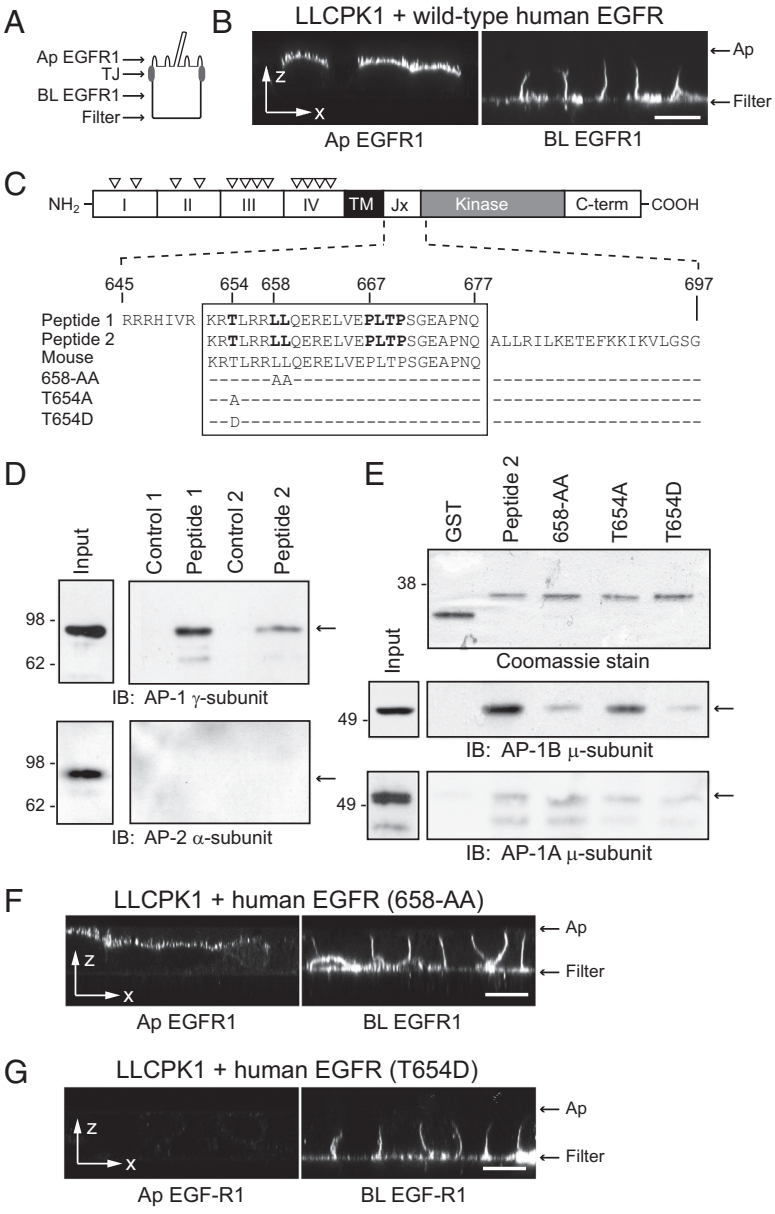

Figure 4. EGFR 658-LL basolateral sorting signal interacts with AP-1B. (A) Human-specific EGFR expression was evaluated by domain-specific EGFR1 staining of nonpermeabilized cells with well-formed tight junctions (TJ). (B) Horizontal x-z optical sections from LLCPK1 cells expressing wild-type human EGFR after domain-specific EGFR1 staining. (C) EGFR protein schematic highlights extracellular region with four subdomains (I–IV) and multiple N-glycosylation sites (▽), transmembrane (TM) domain, and cytoplasmic region with juxtamembrane (Jx), kinase catalytic, and carboxyl terminal (C-term) domains. Amino acid sequences of wild-type (peptide 1 and peptide 2) and mutant (T654A, T654D, and 658-AA) peptides used in pulldown assays are shown beneath the schematic. Critical residues involved in basolateral sorting are highlighted in bold (Hobert *et al.*, 1997; He *et al.*, 2002). Peptide sequences derived from human EGFR (Swiss-Prot: P00533.2) are precisely conserved in mouse EGFR (GenBank: AAA17899.1). (D) Peptides conjugated to Sepharose beads (peptide 1) or GST fusion protein attached to glutathione beads (peptide 2) were incubated with cell fractions enriched for AP complexes, and bound proteins were immunoblotted with AP-specific antibodies. Cell fractions were also incubated with empty Sepharose beads (Control 1) or affinity purified GST protein (Control 2). (E) Top: Coomassie-stained gel of affinity-purified GST fusion proteins. Bottom: GST fusion protein pulldown assays analyzed with a previously published AP-1B μ-subunit specific antibody (Fölsch *et al.*, 1999). (F and G) Horizontal x-z optical sections from LLCPK1 cells expressing human EGFRs with 658-AA (F) or T654D (G) substitutions stained with domain-specific EGFR1. Scale bars, (B, F, and G) 5 μm.

of AP-1B–dependent basolateral cargo (Fölsch *et al.*, 1999). LLCPK1 cells expressing recombinant human EGFR were grown on permeable filter supports and stained with EGFR1 mAb added to the apical or basolateral surface (Figure 4A; Hobert *et al.*, 1997). EGFR1 recognizes a peptide epitope in the extracellular domain of the receptor and is human-specific (Waterfield *et al.*, 1982; Carlin and Knowles, 1984). Human EGFRs were detectable on both membrane domains (Figure 4B), indicating that they follow multiple pathways to the basolateral surface including one regulated by AP-1B. We have reported previously that EGFR polarity is regulated by hierarchical signals including two conserved basolateral sorting motifs located in the juxtamembrane region of the receptor (Figure 4C; Hobert *et al.*, 1997; He *et al.*, 2002). Using in vitro pulldown assays, we demonstrated that EGFR peptides encompassing the dileucine-based 658-LL basolateral sorting motif specifically interacted with AP-1 but not AP-2 involved in clathrin-dependent sorting at the level of the plasma membrane (Figure 4D; Robinson and Bonifacino, 2001). Furthermore this sequence interacted with the epithelial-specific isoform AP-1B in vitro (Figure 4E). Previously characterized dileucine sorting signals require an acidic residue at the −4 position [i.e., D/ExxxL(L/I); Bonifacino and Traub, 2003] for full biological activity. Although the 658-LL motif lacks an acidic residue, Thr654 at the −4 position is a known serine-threonine kinase substrate that could serve a similar role by introducing a negative charge in its phosphorylated state (Hunter *et al.*, 1985; Bagowski *et al.*, 1999). A T654A substitution had a relatively modest effect on AP-1B binding in the pulldown assay (Figure 4E). Contrary to what we expected, in vitro AP-1B binding was essentially eliminated by a T654D phospho-mimetic substitution (Figure 4E). AP-1B binding was also greatly reduced by a 658-AA substitution (Figure 4E). Introduction of the 658-AA substitution to full-length human EGFR did not eliminate basolateral expression in LLCPK1 cells, confirming the existence of a second AP-1B–independent constitutive pathway (Figure 4F). Interestingly, the T654D substitution abolished apical

EGFR expression in LLCPK1 cells, suggesting this mutation offsets μ1B deficiency (Figure 4G). These data indicate EGFR is sorted by at least three mechanisms: AP-1B–dependent and –independent constitutive pathways and an inducible AP-1B–independent pathway regulated by a latent signal involving Thr654. Furthermore, the 658-LL sorting signal does not conform to previously characterized consensus D/ExxxL(L/I) dileucine motifs, suggesting it has unique molecular requirements.

EGFRs Follow Multiple Pathways to the Basolateral Membrane in MDCK Cells

The hypothesis that different EGFR sorting signals mediate trafficking in distinct pathways was further evaluated in MDCK cells, which express μ1B constitutively (Ohno *et al.*, 1999). Permanent MDCK cell lines encoding recombinant human EGFR proteins were subjected to domain-specific EGFR1 staining, demonstrating that wild-type human EGFR and human EGFR with a T654D substitution are enriched on basolateral membranes (Figure 5, A and B). In contrast human EGFR with a 658-AA substitution was detectable on both membrane domains (Figure 5C). All the permanent cell lines displayed normal patterns of ZO-1 and E-cadherin staining, ruling out the possibility that nonpolar human EGFR (658-AA) expression was due to loss of cell–cell junctional contacts. Despite similarities in membrane domain targeting, our data indicate wild-type human EGFR and human EGFR (T654D) traverse distinct basolateral pathways. Receptors with a T654D mutation colocalized with Rab11 subapical compartments (Figure 5D). Interestingly, subapical Rab11 is a marker for AREs involved in lipid raft–independent apical trafficking (Apodaca, 2001; Hoekstra *et al.*, 2004). In contrast, wild-type EGFR was largely excluded from this compartment in MDCK cells (Figure 5E). Differences in basolateral sorting itineraries were not due to variable levels of EGFR protein expression levels (Figure 5F). In addition, wild-type EGFR and EGFR (T654D) exhibited similar metabolic stability after basolateral delivery, with turnover rates of ~1% per h. These data suggest both these ectopic receptors were faithfully recycled to the basolateral

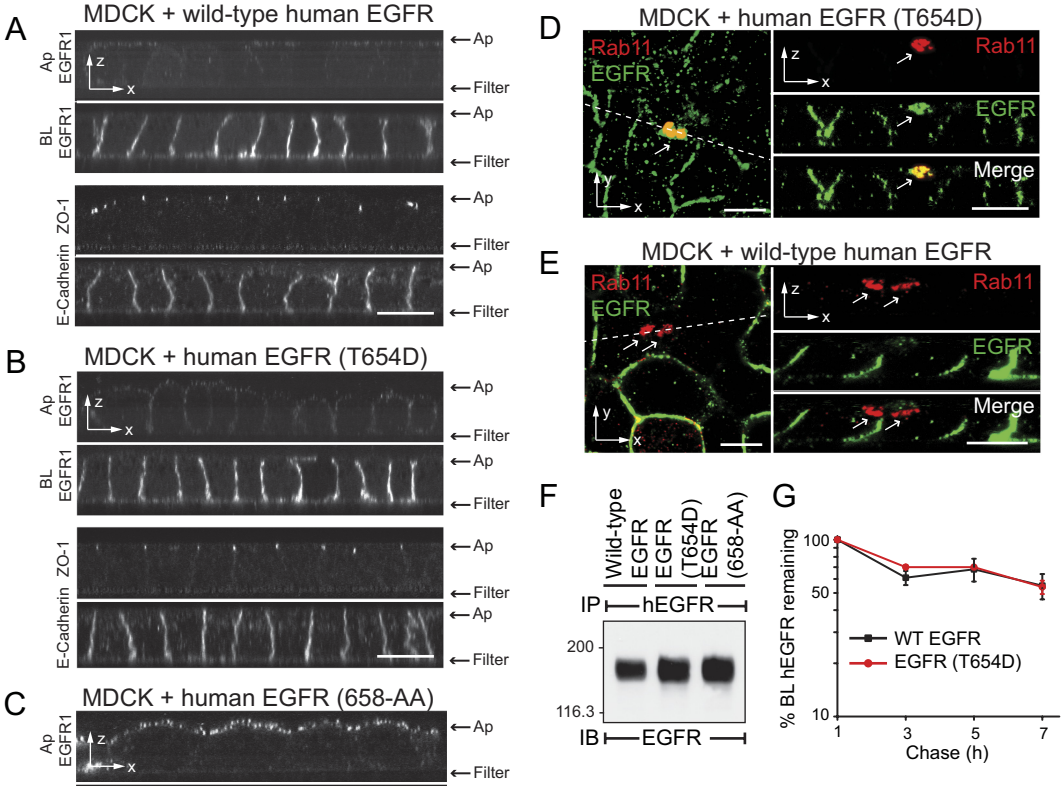

Figure 5. EGFR follows multiple basolateral sorting pathways in MDCK cells. (A–C) Horizontal x-z optical sections from nonpermeabilized MDCK cells expressing wild-type human EGFR (A), human EGFR with a T654D substitution (B), or human EGFR with 658-AA substitution (C), stained with domain-specific EGFR1 (see Figure 4A). Permeabilized cells were also stained with ZO-1 and E-cadherin antibodies. (D and E) Vertical x-y optical sections from representative MDCK cells expressing EGFR with a T654D substitution (D) or wild-type human EGFR (E) costained for Rab11 (red channel) and human EGFR (green channel). Unmerged and merged images from Z-sections indicated by dotted lines are shown to the right. Arrows, Rab11-positive subapical compartments. Scale bars, (A–E) 5 μm. (F) Human-specific EGFR immune complexes from permanent MDCK cell lines expressing recombinant human EGFR proteins listed in the figure were immunoblotted with a second EGFR antibody. (G) Cells were pulse-labeled with ^{35}S-amino acids and then switched to chase media for up to 7 h. Cells were biotinylated at the basolateral surface at times indicated, and biotinylated EGFR immune complexes were recovered by streptavidin affinity purification. EGFR-associated radioactivity was quantified by phosphorstorage autoradioactivity. Data are plotted as the log percent radioactivity remaining compared with the 1-h time point, which was set to 100, as a function of time (mean ± SEM, n = 3).

membrane after constitutive EGFR internalization (Figure 5G). Altogether these data confirm results obtained in μ1B-null LLCPK1 cells that EGFRs are constitutively transported to the basolateral membrane by multiple pathways. They also indicate receptors in the inducible Thr654-dependent pathway traverse Rab11-positive subapical compartments en route to the basolateral membrane.

Recovery of Basolateral EGFR Expression in Cystic Cells by Activation of Latent Thr654-dependent Signal

Studies to this point have uncovered multiple routes for polarized EGFR trafficking. These findings raise the possibility that the EGFR cellular phenotype associated with PKD could be overcome by activating an alternative basolateral sorting pathway. This hypothesis was tested by analyzing the distribution of human EGFRs with sorting signal mutations in permanent cystic cell lines. Nonpermeabilized cells were stained with domain-specific EGFR1 (see Figure 4A). Cells on replicate filters were stained for CD73 to verify that ectopic human EGFR expression does not perturb lipid raft–dependent apical sorting. Cells were also stained for ZO-1 and E-cadherin as indicators of cell polarity. Wild-type human EGFR was detectable on both membrane surfaces (Figure 6A), confirming results in Figure 3A obtained with permeabilized cells. Similar to the wild-type receptor, human EGFR with a 658-AA substitution was also present on both membrane surfaces in cystic cells (Figure 6B). However, human EGFR with the T654D substitution was targeted exclusively to basolateral membranes (Figure 6C). In addition to microscopy studies, human EGFR membrane domain delivery was examined in pulse-chase experiments (Figure 6D). In contrast to Figure 3G, these studies were carried out without synchronizing newly synthesized molecules in the Golgi. Although wild-type human EGFR and human EGFR (658-AA) both exhibited nonpolar delivery, human EGFR (658-AA) appeared on the apical surface ~30 min before wild-type human EGFR consistent with subtle differences in delivery pathways. In contrast to these two receptor molecules, human EGFR (T654D) was delivered directly to the basolateral surface in cystic cells. EGFR residue Thr654 is a known protein kinase C (PKC) substrate (Hunter *et al.*, 1985), suggesting that PKC might activate the latent signal and restore basolateral localization of wild-type EGFR in cystic cells. Cystic cells were treated with PMA that is known to activate the major PKC isoforms expressed in adult renal collecting duct to test this hypothesis (Redling *et al.*, 2004).

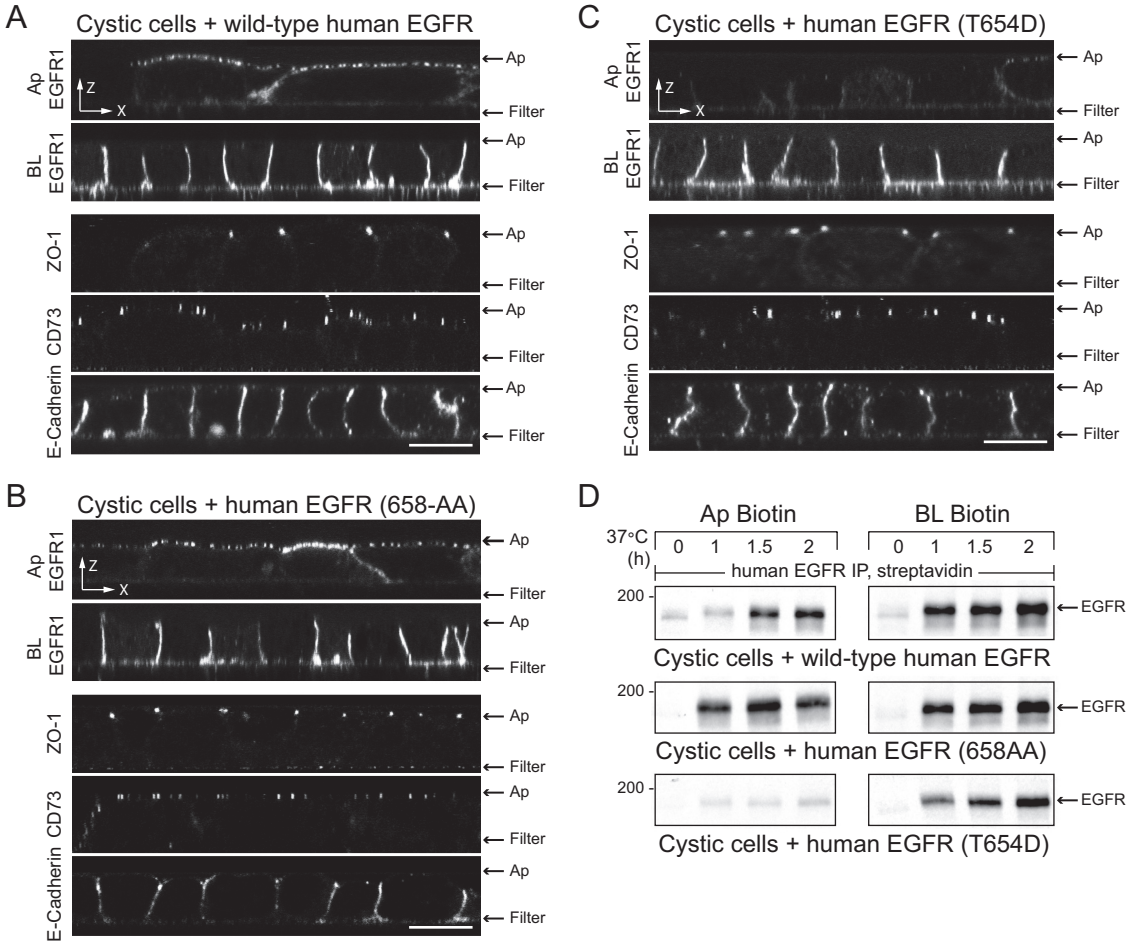

Figure 6. T654D mutation reconstitutes basolateral EGFR expression in cystic cells. (A–C) Horizontal x-z confocal optical sections from cystic cells expressing wild-type human EGFR (A) or human EGFR with 658-AA (B) or T654D (C) substitutions stained with EGFR1 according to Figure 4A, or antibodies to epithelial cell markers. Scale bars, 5 μm. (D) Cells were pulse-labeled with ^{35}S-Express Protein Labeling Mix for 15 min and biotinylated immediately or after a 37°C incubation period in chase media. Radiolabeled human EGFR immune complexes purified by streptavidin affinity chromatography were detected by fluorography.

Although PMA rapidly induced Thr654 phosphorylation in cells expressing wild-type EGFR but not EGFR (T654D) (Supplemental Figure 1A), this treatment had no discernable effect on apical EGFR expression in cystic cells (Supplemental Figure 1B). Altogether these data indicate wild-type EGFR and EGFR (658-AA) arrive at the apical membrane via kinetically distinct pathways, they also suggest that receptors with a T654D substitution traverse a novel PMA-insensitive basolateral sorting pathway via Rab11-positive AREs that is unaffected by the disease allele.

EGFR Colocalizes with Rab11-positive Subapical Compartments in Cystic Cells

Normal and cystic cells expressing human EGFRs were costained with antibodies to Rab11 and the human receptor. Our data indicate that wild-type human EGFR is excluded from Rab11-positive subapical compartments in normal cells (Figure 7, A and D), in contrast to cystic cells, which exhibit substantial overlap of these two markers (Figure 7, B and E). Although these compartments had a tubulovesicular appearance in normal cells similar to the structures identified in MDCK cells (Figure 5, E and F), the Rab11-positive subapical compartments appeared more punctuate in cystic cells. Similar to data from MDCK cells (Figure 5E), human EGFR (T654D) also colocalized with Rab11-positive subapical compartments in cystic cells (Figure 7, C and F). E-cadherin, which requires Rab11 and functional AREs for normal basolateral trafficking (Desclozeaux *et al.*, 2008), localized to similar Rab11-positive subapical compartments in all three of the cell lines (Figure 7, D–F). Altogether these data indicate wild-type human EGFR and human EGFR (T654D) transit Rab11-positive subapical compartments resembling E-cadherin ARE sorting intermediates in the cystic cells. However, in contrast to wild-type EGFR that missorts to the apical membrane, EGFR (T654D) trafficking to the basolateral membrane is unaffected by the disease allele.

DISCUSSION

Our studies indicate that newly synthesized EGFRs follow at least two constitutive basolateral sorting pathways in renal epithelial cells. One pathway is mediated by direct interaction between a highly conserved unconventional EGFR dileucine motif 658-LL and AP-1B. Similar to other cargoes, AP-1B probably sorts EGFRs in CREs (route B1 in Figure 8; Gonzalez and Rodriguez-Boulan, 2009). An AP-1B–independent constitutive pathway was also identified. Although the molecular basis for this alternative route is not yet known, it may involve the conserved EGFR basolateral signal 667-PLTP that binds SH3-domain ligands in vitro (He *et al.*, 2002; Hake *et al.*, 2008). One current model postulates AP-1B–independent trafficking is mediated by an unknown clathrin adaptor that sorts cargo directly from the TGN to the plasma membrane (route B2). Alternatively, cargo may be sorted independent of clathrin via BSEs (route B3; Gonzalez and Rodriguez-Boulan, 2009). We have also unmasked a latent basolateral pathway that transits Rab11-positive subapical compartments independent of AP-1B (route B4), by replacing EGFR residue Thr654 with a negatively charged aspartic acid. Based on subcellular localization, Rab11 staining, and

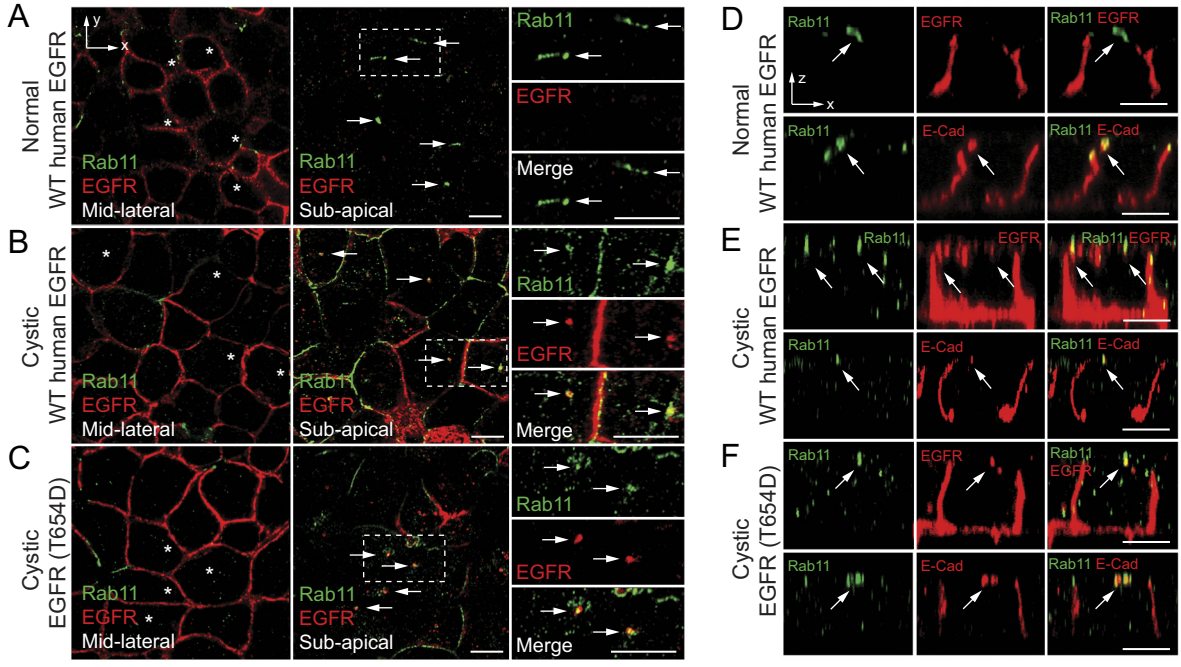

Figure 7. EGFR colocalizes with Rab11-positive subapical compartments in cystic cells. (A–C) Vertical x-y confocal optical sections from the midlateral (left panels) or subapical (middle panels) regions of normal cells expressing wild-type human EGFR (A), cystic cells expressing wild-type human EGFR (B), or cystic cells expressing human EGFR with a T654D substitution (C) costained for Rab11 (green channel) and human EGFR (red channel). Panels to far right are magnified images of individual and merged channels from boxed areas in subapical sections. Arrows, Rab11-positive subapical compartments. Asterisks in midlateral sections denote cells with Rab11-positive subapical compartments. (D–F) Individual and merged channels of horizontal x-z confocal sections from normal cells expressing wild-type human EGFR (D), cystic cells expressing wild-type human EGFR (E), or cystic cells expressing human EGFR with a T654D substitution (F) costained for Rab11 (green channels in both sets of panels) and either human EGFR or E-cadherin (red channels in top or bottom panels, respectively). Arrows denote Rab11-positive subapical compartments. Scale bars, 5 μm.

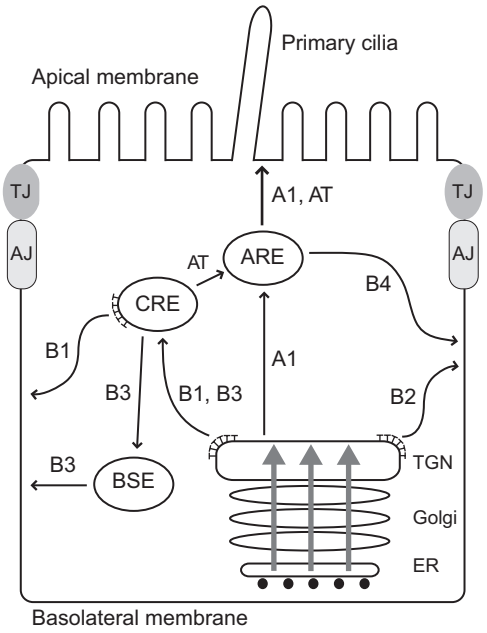

Figure 8. The model depicts a variety of routes followed by newly synthesized EGFR in polarized renal cells. EGFRs are transported to the CRE where they undergo AP-1B–dependent transport to the basolateral membrane via route B1. EGFR also follows an AP-1B–independent pathway that may bypass CREs using a direct route from the TGN to the basolateral membrane (B2). Alternatively this pathway may involve a hypothetical route from CREs to BSEs (B3). Introduction of an aspartic acid residue for Thr654 unmasks a third route that traverses AREs en route to the basolateral membrane (B4). Receptors in this pathway may reach AREs by a direct route from the TGN (A1) or via a CRE intermediate (AT). The B1 pathway is impaired in μ1B-null LLCPK1 cells as well as cystic cells from the BPK model with constitutive μ1B expression. The B4 pathway bypasses AP-1B and reconstitutes polar EGFR expression in both cell types. Apically missorted EGFRs probably follows the N-glycan–dependent A1 pathway rather than the lipid raft–dependent pathway that involves ASE intermediates (not shown). Gray arrows indicate polarized protein cargoes that may be presorted in the ER or Golgi. AJ, adherens junction; TJ, tight junction; ⊤, clathrin.

the presence of E-cadherin in similar structures, these compartments are probably AREs (Apodaca, 2001; Hoekstra *et al.*, 2004). At present it is unclear if EGFR (T654D) receptors are targeted to AREs directly (route A1) or via CREs (route AT). Interestingly, the EGFR T654D substitution inhibits AP-1B binding in vitro. This finding raises the possibility that T654D silences the AP-1B signal in addition to activating a novel basolateral sorting signal.

The 658-AA mutation does not exacerbate the EGFR disease phenotype, indicating that the BPK mutant allele specifically interferes with the constitutive AP-1B pathway. However, cystic cells have functional AP-1B machinery, suggesting these cells may be missing an essential EGFR-specific regulatory protein. Other membrane proteins require cargo-specific subunits of the exocyst complex utilized by AP-1B vesicles (Fölsch, 2005). For example, Rho family GTPase TC10 is required for exocyst-mediated membrane fusion of certain cargo as well as membrane expansion in developing neurons (Chiang *et al.*, 2001; Cuadra *et al.*, 2004; Cheng *et al.*, 2005; Dupraz *et al.*, 2009). It is also possible that excess AP-1B expressed in cystic cells partially uncouples the AP-1B pathway from a rate-limiting regulatory protein needed for proper EGFR basolateral sorting. Without the putative regulatory protein, EGFRs may be recognized by machinery involved in transporting *N*-glycan dependent cargoes from CRE to apical membrane (route AT; Hobert *et al.*, 1997).

The disease allele does not impair T654D-dependent EGFR basolateral transport, suggesting that the negative charge activates a latent signal that overcomes AP-1B–dependent sorting abnormalities. It remains to be determined if the T654D-dependent pathway is activated by phosphorylation. Although PMA-sensitive PKC isoforms were tentatively ruled out, other serine/threonine kinases have critical roles in polarized sorting. For example, atypical PKC regulates PAR proteins involved in early cell polarization events (Goldstein and Macara, 2007), and PKD mediates basolateral transport carrier fission from TGN (Yeaman *et al.*, 2004). However, neither of these kinases appears to modify specific membrane protein cargo. Previous studies indicate the EGFR sequence containing Thr654 forms an amphiphilic helix that binds strongly to membrane-mimetic micelles in vitro (Choowongkomon *et al.*, 2005). Introduction of a negative charge disrupts the helical structure and dramatically alters overall EGFR juxtamembrane conformation. The EGFR juxtamembrane region has multiple protein interaction partners including calmodulin and phosphoinositide kinases (Cochet *et al.*, 1991; Martin-Nieto and Villalobo, 1998) that could conceivably trigger localized conformational changes or phosphoinositide metabolism independent of Thr654 phosphorylation. E-cadherin is also routed basolaterally via Rab11-positive AREs by an AP-1B–independent pathway (Desclozeaux *et al.*, 2008). Interestingly this pathway involves an unconventional dileucine-based sorting signal lacking an acidic residue at the −4 position (Miranda *et al.*, 2001). ARE-dependent E-cadherin basolateral sorting is required for lumen formation during epithelial morphogenesis (Desclozeaux *et al.*, 2008), raising the possibility the latent Thr654-dependent EGFR signal has a similar role during development or tissue repair.

Epithelial cell polarity is also regulated by polarized recycling from endosomes. The hypothesis that EGFRs do not properly engage AP-1B in cystic cells implies these cells may also be defective for EGFR recycling from CREs. However, constitutive EGFR internalization is relatively slow (Wiley *et al.*, 1991) and any contribution of recycling pathways to the overall PKD phenotype may be modest. Although we cannot formally exclude the possibility that EGFRs also missort postendocytically, our data indicate the cystic EGFR phenotype primarily involves defective sorting in the secretory pathway.

Identification of the AP-1B subunit(s) that recognize the unconventional EGFR dileucine motif is an important future direction for these studies. On the one hand, the EGFR interaction could involve unique carboxyl terminal sequences in the μ1B subunit that are thought to protrude from intact AP1 complexes and to be important for interactions with sorting signals (Ohno *et al.*, 1999). Alternatively, divergent sequences in their amino-terminal domains may affect how μ1B interacts with other adaptor subunits. These differences could be important if the 658-LL interaction is mediated by AP-1B hemi-complexes involving the μ1B subunit (Owen *et al.*, 2004).

It will also be interesting to determine the link between defective AP-1B–dependent EGFR sorting and the primary gene defect in the BPK model. *Drosophila* Bicc-1 binds a subunit of the CCR4-NOT deadenylation complex responsible for shortening of specific mRNAs during early embryonic patterning (Chicoine *et al.*, 2007). Recent data indicate the *Drosophila* protein regulates endoplasmic reticulum (ER)

exit site homeostasis necessary for normal protein sorting and that specific proteins become trapped in aberrant exit site compartments, leading to defective exocytosis in *Bicc-1*-null embryos (Kugler *et al.*, 2009). Although the EGFR sorting defect involves inaccurate incorporation into post-Golgi transport vesicles, a growing number of studies indicate protein cargo are presorted in the ER or bypass the Golgi altogether (Prydz *et al.*, 2007; Tveit *et al.*, 2009). Besides EGFR, the BPK mutant allele could also block trafficking of the putative regulatory protein required for EGFR sorting by AP-1B. The ER is emerging as a common target for PKD susceptibility gene products. Recent data indicate PKD1 influences the shape and localization of both the microtubule network and the ER (Gao *et al.*, 2009), and PKD2 is an abundant ER protein that functions as a novel intracellular Ca^{2+} release channel (Koulen *et al.*, 2002; Li *et al.*, 2005).

Another novel finding from these studies is that EGFR-dependent signaling is perturbed at both membrane surfaces in cystic cells. It is conceivable the disease allele modulates EGFR signaling by causing an alternative distribution in basolateral membrane subdomains through reduced incorporation into AP-1B transport vesicles. This hypothesis is consistent with the idea that overlapping but separate routes to the same membrane domain allow different epithelial cell types to carry out unique physiological functions. Furthermore AP-1B–independent routes for some cargo develop after cells have polarized, in contrast to AP-1B, which has a prominent role in newly polarized cells, suggesting these pathways have distinct roles during development or differentiation (Gonzalez and Rodriguez-Boulan, 2009). Interestingly ERK1/ERK2 is hyperactivated in cystic kidneys, and inhibition of this pathway slows disease progression in PKD mouse models (Yamaguchi *et al.*, 2004; Veizis and Cotton, 2005). Our data suggest that imbalanced EGFR signaling from both membrane domains contributes to hyperactive ERK1/ERK2 responses associated with PKD.

Multiple sorting pathways provide for EGFR membrane plasticity important for tissue homeostasis. The BPK disease allele appears to selectively interfere with AP-1B–dependent EGFR sorting, suggesting EGFR polarity could be reconstituted if receptors were diverted away from this pathway. In addition, recognition by alternative basolateral sorting pathways could fine-tune EGFR signaling and restrict cell proliferation, contributing to cystogenesis. Our data also suggest a novel role for *Bicc-1* disease-specific transcript in AP-1B–dependent EGFR basolateral transport that may also yield novel insights to other ARPKD susceptibility genes.

ACKNOWLEDGMENTS

We thank Edward Greenfield (Department of Orthopedics, Case Western Reserve University) for the gift of GAPDH primers, William Sweeney and Ellis Avner for many useful discussions, Brad Fairfield for technical assistance with manuscript preparation, and other members of the Carlin laboratory for reviewing the manuscript. This work was supported by Public Health Service Grants P50 DK54178 (C.R.C. and C.U.C.) and R01GM081498 (C.R.C.). S.R. was supported in part by National Institutes of Health Grant T32 HL-007415.

REFERENCES

Apodaca, G. (2001). Endocytic traffic in polarized epithelial cells: role of the actin and microtubule cytoskeleton. Traffic *2*, 149–159.

Bagowski, C. P., Stein-Gerlach, M., Choidas, A., and Ullrich, A. (1999). Cell-type specific phosphorylation of threonines T654 and T669 by PKD defines the signal capacity of the EGF receptor. EMBO J. *18*, 5567–5576.

Bonifacino, J., and Traub, L. (2003). Signals for sorting of transmembrane proteins to endosomes and lysosomes. Annu. Rev. Biochem. *72*, 395–434.

Brown, D. A., Crise, B., and Rose, J. K. (1989). Mechanisms of membrane anchoring affects polarized expression of two proteins in MDCK cells. Science *245*, 1499–1501.

Brown, D. A., and Rose, J. K. (1992). Sorting of GPI-anchored proteins to glycolipid-enriched membrane subdomains during transport to the apical cell surface. Cell *68*, 533–544.

Brown, N. E., and Murcia, N. S. (2003). Delayed cystogenesis and increased ciliogenesis associated with the re-expression of polaris in Tg737 mutant mice. Kidney Int. *63*, 1220–1229.

Bryant, D. M., and Mostov, K. E. (2008). From cells to organs: building polarized tissue. Nat. Rev. Mol. Cell Biol. *9*, 887–901.

Carlin, C. R., and Knowles, B. B. (1984). Biosynthesis of the epidermal growth factor receptor in human epidermoid carcinoma-derived A431 cells. J. Biol. Chem. *259*, 7902–7908.

Carlin, C. R., and Knowles, B. B. (1986). Biosynthesis and glycosylation of the epidermal growth factor receptor in human tumor-derived cell lines A431 and Hep 3B. Mol. Cell. Biol. *6*, 257–264.

Cheng, J., Wang, H., and Guggino, W. B. (2005). Regulation of cystic fibrosis transmembrane regulator trafficking and protein expression by a Rho family small GTPase TC10. J. Biol. Chem. *280*, 3731–3739.

Chiang, S.-H., Baumann, C. A., Kanzaki, M., Thurmond, D. C., Watson, R. T., Neudauer, C. L., Macara, I. G., Pessin, J. E., and Saltiel, A. R. (2001). Insulin-stimulated GLUT4 translocation requires the CAP-dependent activation of TC10. Nature *410*, 944–948.

Chicoine, J., Benoit, P., Gamberi, C., Paliouras, M., Simonelig, M., and Lasko, P. (2007). Bicaudal-C recruits CCR4-NOT deadenylase to target mRNAs and regulates oogenesis, cytoskeletal organization, and its own expression. Dev. Cell *13*, 691–704.

Choowongkomon, K., Carlin, C., and Sonnichsen, F. (2005). A structural model for the membrane-bound form of the juxtamembrane domain of the epidermal growth factor receptor. J. Biol. Chem. *280*, 24043–24052.

Cianciola, N. L., Crooks, D., Shah, A. H., and Carlin, C. (2007). A tyrosine-based signal plays a critical role in the targeting and function of adenovirus RIDα protein. J. Virol. *81*, 10437–10450.

Cochet, C., Filhol, O., Payrastre, O., Hunter, T., and Gill, G. N. (1991). Interaction between the epidermal growth factor receptor and phosphoinositide kinases. J. Biol. Chem. *266*, 637–644.

Cogswell, C., Price, S. J., Hou, X., Guay-Woodford, L. M., Flaherty, L., and Bryda, E. C. (2003). Positional cloning of jcpk/bpk locus of the mouse. Mamm. Genome *14*, 242–249.

Crepaldi, T., Pollack, A., Prat, M., Zborek, A., Mostov, K., and Comoglio, P. (1994). Targeting of the SF/HGF receptor to the basolateral domain of polarized epithelial cells. J. Cell Biol. *125*, 313–320.

Cresawn, K. O., Potter, B. A., Oztan, A., Guerriero, C. J., Ihrke, G., Goldenring, J. R., Apodaca, G., and Weisz, O. A. (2007). Differential involvement of endocytic compartments in the biosynthetic traffic of apical proteins. EMBO J. *26*, 3737–3748.

Crooks, D., Kil, S. J., McCaffery, J. M., and Carlin, C. (2000). E3-13.7 integral membrane proteins encoded by human adenoviruses alter epidermal growth factor receptor trafficking by interacting directly with receptors in early endosomes. Mol. Biol. Cell *11*, 3559–3572.

Cuadra, A. E., Kuo, S.-H., Kawasaki, Y., Bredt, D. S., and Chetkovich, D. M. (2004). AMPA receptor synaptic targeting regulated by Stargazin interactions with the Golgi-resident PDZ protein nPIST. J. Neurosci. *24*, 7491–7502.

Desclozeaux, M., Venturato, J., Wylie, F. G., Kay, J. G., Joseph, S. R., Le, H. T., and Stow, J. L. (2008). Active Rab11 and functional recycling endosome are required for E-cadherin trafficking and lumen formation during epithelial morphogenesis. Am. J. Physiol. Cell Physiol. *295*, C545–C556.

Dupraz, S., Grassi, D., Bernis, M. E., Sosa, L., Bisbal, M., Gastaldi, L., Jausoro, I., Caceres, A., Pfenninger, K. H., and Quiroga, S. (2009). The TC10-Exo70 complex is essential for membrane expansion and axonal specification in developing neurons. J. Neurosci. *29*, 13292–13301.

Fischer, E., and Pontoglio, M. (2009). Planar cell polarity and cilia. Semin. Cell Dev. Biol. *20*, 998–1005.

Fölsch, H. (2005). The building blocks for basolateral vesicles in polarized epithelial cells. Trends Cell Biol. *15*, 222–228.

Fölsch, H., Ohno, H., Bonifacino, J. S., and Mellman, I. (1999). A novel clathrin adaptor complex mediates basolateral targeting in polarized epithelial cells. Cell *99*, 189–198.

Gan, Y., McGraw, T. E., and Rodriguez-Boulan, E. (2002). The epithelial-specific adaptor AP1B mediates post-endocytic recycling to the basolateral membrane. Nat. Cell Biol. *4*, 605–609.

Gao, H., Sellin, L. K., Pütz, M., Nickel, C., Imgrund, M., Gerke, P., Nitschke, R., Walz, G., and Kramer-Zucker, A. G. (2009). A short carboxy-terminal domain of polycystin-1 reorganizes the microtubular network and the endoplasmic reticulum. Exp. Cell Res. *315*, 1157–1170.

Goldstein, B., and Macara, I. G. (2007). The PAR proteins: fundamental players in animal cell polarization. Dev. Cell *13*, 609–622.

Gonzalez, A., and Rodriguez-Boulan, E. (2009). Clathrin and AP1B: key roles in basolateral trafficking through trans-endosomal routes. FEBS Lett. *583*, 3784–3795.

Goodyer, P. R., Kachra, Z., Bell, C., and Rozen, R. (1988). Renal tubular cells are potential targets for epidermal growth factor. Am. J. Physiol. Renal Physiol. *255*, F1191–F1196.

Grantham, J. J. (2003). Lillian Jean Kaplan International Prize for Advancement in the Understanding of Polycystic Kidney Disease. Kidney Int. *64*, 1157–1162.

Guay-Woodford, L. M. (2003). Murine models of polycystic kidney disease: molecular and therapeutic insights. Am. J. Physiol. Renal Physiol. *285*, F1034–F1049.

Hake, M. J., Choowongkomon, K., Kostenko, O., Carlin, C. R., and Sönnichsen, F. D. (2008). Specificity determinants of a novel Nck interaction with the juxtamembrane domain of the epidermal growth factor receptor. Biochemistry *47*, 3096–3108.

Harlow, E., and Lane, D. (1988). Antibodies: A Laboratory Manual, Cold Spring Harbor, NY: Cold Spring Harbor Laboratory Press.

Harris, P. C., and Torres, V. E. (2009). Polycystic kidney disease. Annu. Rev. Med. *60*, 321–337.

He, C., Hobert, M., Friend, L., and Carlin, C. (2002). The epidermal growth factor receptor juxtamembrane domain has multiple basolateral plasma membrane localization determinants, including a dominant signal with a polyproline core. J. Biol. Chem. *277*, 38284–38293.

Heike, F., Polly, E. M., and Ora, A. W. (2009). Taking the scenic route: biosynthetic traffic to the plasma membrane in polarized epithelial cells. Traffic *10*, 972–981.

Hiesberger, T., Gourley, E., Erickson, A., Koulen, P., Ward, C. J., Masyuk, T. V., Larusso, N. F., Harris, P. C., and Igarashi, P. (2006). Proteolytic cleavage and nuclear translocation of fibrocystin is regulated by intracellular Ca^{2+} and activation of protein kinase C. J. Biol. Chem. *281*, 34357–34364.

Hobert, M., and Carlin, C. (1995). Cytoplasmic juxtamembrane domain of human EGF receptor is required for basolateral localization in MDCK cells. J. Cell. Physiol. *162*, 434–446.

Hobert, M., Friend, L., and Carlin, C. (1999). Regulation of EGF signaling by cell polarity in MDCK kidney epithelial cells. J. Cell. Physiol. *181*, 330–341.

Hobert, M. E., Kil, S., and Carlin, C. R. (1997). The cytoplasmic juxtamembrane domain of the epidermal growth factor receptor contains a novel autonomous basolateral sorting signal. J. Biol. Chem. *272*, 32901–32909.

Hoekstra, D., Tyteca, D., and van Jzendoorn, S.C.D. (2004). The subapical compartment: a traffic center in membrane polarity development. J. Cell Sci. *117*, 2183–2192.

Hunter, T., Ling, N., and Cooper, J. A. (1985). Protein kinase C phosphorylation of the EGF receptor at a threonine residue close to the cytoplasmic face of the plasma membrane. Nature *311*, 480–483.

Hunziker, W., Mâle, P., and Mellman, I. (1990). Differential microtubule requirements for transcytosis in MDCK cells. EMBO J. *9*, 3515–3525.

Igarashi, P., and Somlo, S. (2002). Genetics and pathogenesis of polycystic kidney disease. J. Am. Soc. Nephrol. *13*, 2384–2398.

International Consortium for Polycystic Kidney Disease. (1995). Polycystic kidney disease: the complete sequence of the PKD1 gene and its protein. Cell *81*, 289–298.

Jensen, C. G., Davison, E. A., Bowser, S. S., and Rieder, C. L. (1987). Primary cilia cycle in PtK1 cells: effects of colcemid and taxol on cilia formation and resorption. Cell Motil. Cytoskelet. *7*, 187–197.

Kaimori, J. Y., Nagasawa, Y., Menezes, L. F., Garcia-Gonzalez, M. A., Deng, J., Imai, E., Onuchic, L. F., Guay-Woodford, L. M., and Germino, G. G. (2007). Polyductin undergoes notch-like processing and regulated release from primary cilia. Hum. Mol. Genet. *16*, 942–956.

Kil, S. J., Hobert, M. E., and Carlin, C. (1999). A leucine-based determinant in the EGF receptor juxtamembrane domain is required for the efficient transport of ligand-receptor complexes to lysosomes. J. Biol. Chem. *274*, 3141–3150.

Koulen, P., Cai, Y., Geng, L., Maeda, Y., Nishimura, S., Witzgall, R., Ehrlich, B. E., and Somlo, S. (2002). Polycystin-2 is an intracellular calcium release channel. Nat. Cell Biol. *4*, 191–197.

Kriz, W., and Kaissing, B. (2008). Structural and functional organization of the kidney. In: Seldin and Giebisch's The Kidney, ed. R. Alpern and S. Hebert, San Diego: Academic Press, 479–564.

Kugler, J. M., Chicoine, J., and Lasko, P. (2009). Bicaudal-C associates with a Trailer Hitch/Me31B complex and is required for efficient Gurken secretion. Dev. Biol. *328*, 160–172.

Li, Y., Wright, J. M., Qian, F., Germino, G. G., and Guggino, W. B. (2005). Polycystin 2 interacts with type I inositol 1,4,5-trisphosphate receptor to modulate intracellular Ca^{2+} signaling. J. Biol. Chem. *280*, 41298–41306.

Lisanti, M., LeBivic, A., Saltiel, A., and Rodriguez-Boulan, E. (1990). Preferred apical distribution of glycosyl-phosphatidylinositol (GPI) anchored proteins: a highly conserved feature of the polarized epithelial cell phenotype. J. Membr. Biol. *113*, 155–167.

Martin-Nieto, J., and Villalobo, A. (1998). The human epidermal growth factor receptor contains a juxtamembrane calmodulin-binding site. Biochemistry *37*, 227–236.

Mellman, I., and Nelson, W. J. (2008). Coordinated protein sorting, targeting and distribution in polarized cells. Nat. Rev. Mol. Cell Biol. *9*, 833–845.

Miranda, K. C., Khromykh, T., Christy, P., Le, T. L., Gottardi, C. J., Yap, A. S., Stow, J. L., and Teasdale, R. D. (2001). A dileucine motif targets E-cadherin to the basolateral cell surface in Madin-Darby canine kidney and LLC-PK1 epithelial cells. J. Biol. Chem. *276*, 22565–22572.

Mochizuki, T., *et al.* (1996). PKD2, a gene for polycystic kidney disease that encodes an integral membrane protein. Science *272*, 1339–1342.

Nauta, J., Ozawa, Y., Sweeney, W. E., Rutledge, J. C., and Avner, E. D. (1993). Renal and biliary abnormalities in a new murine model of autosomal recessive polycystic kidney disease. Pediatr. Nephrol. *7*, 163–172.

Nelson, W. J. (2008). Regulation of cell-cell adhesion by the cadherin-catenin complex. Biochem. Soc. Trans. *36*, 149–155.

Nelson, W. J., and Rodriguez-Boulan, E. (2004). Unravelling protein sorting. Nat. Cell Biol. *6*, 282–284.

Ohno, H., Tomemori, T., Nakatsu, F., Okazaki, Y., Aguilar, R. C., Foelsch, H., Mellman, I., Saito, T., Shirasawa, T., and Bonifacino, J. S. (1999). Mu1B, a novel adaptor medium chain expressed in polarized epithelial cells. FEBS Lett. *449*, 215–220.

Onuchic, L. F., *et al.* (2002). PKHD1, the polycystic kidney and hepatic disease 1 gene (PKHD1) encodes a novel large protein containing multiple IPT domains and PbH1 repeats. Am. J. Hum. Genet. *70*, 1305–1317.

Owen, J., Collins, B. M., and Evans, P. R. (2004). Adaptors for clathrin coats: structure and function. Annu. Rev. Cell Dev. Biol. *20*, 153–191.

Prydz, K., Dick, G., and Tveit, H. (2007). How many ways through the Golgi maze? Traffic *9*, 299–304.

Redling, S., Pfaff, I. L., Leitges, M., and Vallon, V. (2004). Immunolocalization of protein kinase C isoenzymes α, βI, βII, δ, and ε in mouse kidney. Am. J. Physiol. Renal Physiol. *287*, F289–F298.

Richards, W. G., Sweeney, W. E., Yoder, B. K., Wilkinson, J. E., Woychik, R. P., and Avner, E. D. (1998). Epidermal growth factor receptor activity mediates renal cyst formation in polycystic kidney disease. J. Clin. Invest. *101*, 935–939.

Robinson, M. S. (1993). Assembly and targeting of adaptin chimeras in transfected cells. J. Cell Biol. *123*, 67–77.

Robinson, M. S., and Bonifacino, J. S. (2001). Adaptor-related proteins. Curr. Opin. Cell Biol. *13*, 444–453.

Rodriguez-Boulan, E., Kreitzer, G., and Musch, A. (2005). Organization of vesicular trafficking in epithelia. Nat. Rev. Mol. Cell Biol. *6*, 233–247.

Sack, E., and Talor, Z. (1988). High affinity binding sites for epidermal growth factor (EGF) in renal membranes. Biochem. Biophys. Res. Comm. *154*, 312–317.

Stevenson, B. R., Siliciano, J. D., Mooseker, M. S., and Goodenough, D. A. (1986). Identification of ZO-1, a high molecular weight polypeptide associated with the tight junction (*zonula occludens*) in a variety of epithelia. J. Cell Biol. *103*, 755–766.

Strohmeier, G., Lencer, W., Patapoff, T., Thompson, L., Carlson, S., Moe, S., Carnes, D., Mrsny, R., and Madara, J. (1997). Surface expression, polarization, and functional significance of CD73 in human intestinal epithelia. J. Clin. Invest. *99*, 2588–2601.

Sweeney, W., and Avner, E. (2006). Molecular and cellular pathophysiology of autosomal recessive polycystic kidney disease (ARPKD). Cell Tissue Res. *326*, 671–685.

Sweeney, W. E., Chen, Y., Nakanishi, K., Frost, P., and Avner, E. D. (2000). Treatment of polycystic kidney disease with a novel tyrosine kinase inhibitor. Kidney Int. *57*, 33–40.

Sweeney, W. E., Jr., Kusner, L., Carlin, C. R., Chang, S., Futey, L., Cotton, C. U., Dell, K. M., and Avner, E. D. (2001). Phenotypic analysis of conditionally immortalized cells isolated from the BPK model of ARPKD. Am. J. Physiol. Cell Physiol. *281*, C1695–C1705.

Sweeney, W. E., Jr., von Vigier, R. O., Frost, P., and Avner, E. D. (2008). Src inhibition ameliorates polycystic kidney disease. J. Am. Soc. Nephrol. *19*, 1331–1341.

Tan, C. M., Nickols, H. H., and Limbird, L. E. (2003). Appropriate polarization following pharmacological rescue of V2 vasopressin receptors encoded by X-linked nephrogenic diabetes insipidus alleles involves a conformation of the receptor that also attains mature glycosylation. J. Biol. Chem. *278*, 35678–35686.

The American Consortium for PKD1. (1995). Analysis of the genomic sequence for the autosomal dominant polycystic kidney disease (PKD1) gene and its protein. Hum. Mol. Genet. *4*, 575–582.

Torres, V., Sweeney, W., Wang, X., Qian, Q., Harris, P., Frost, P., and Avner, E. (2003). EGF receptor tyrosine kinase inhibition attenuates the development of PKD in Han:SPRD rats. Kidney Int. *64*, 1573–1579.

Torres, V. E., and Harris, P. C. (2006). Mechanisms of disease: autosomal dominant and recessive polycystic kidney diseases. Nat. Clin. Pract. Nephrol. *2*, 40–55.

Tveit, H., Akslen, L.K.A., Fagereng, G. L., Tranulis, M. A., and Prydz, K. (2009). A secretory Golgi bypass route to the apical surface domain of epithelial MDCK cells. Traffic *10*, 1685–1695.

Veizis, E. I., Carlin, C. R., and Cotton, C. U. (2004). Decreased amiloride-sensitive Na^+ absorption in collecting duct principal cells isolated from BPK ARPKD mice. Am. J. Physiol. Renal Physiol. *286*, F244–F254.

Veizis, I. E., and Cotton, C. U. (2005). Abnormal EGF-dependent regulation of sodium absorption in ARPKD collecting duct cells. Am. J. Physiol. Renal Physiol. *288*, F474–F482.

Ward, C. J., *et al.* (2002). The gene mutated in autosomal recessive polycystic kidney disease encodes a large, receptor-like protein. Nat. Genet. *30*, 1–11.

Ward, C. J., *et al.* (2003). Cellular and subcellular localization of the ARPKD protein; fibrocystin is expressed on primary cilia. Hum. Mol. Genet. *12*, 2703–2710.

Waterfield, M. D., Mayes, E.L.V., Stroobant, P., Bennet, P.L.P., Young, S., Goodfellow, P. N., Banting, G. S., and Ozanne, B. (1982). A monoclonal antibody to the human epidermal growth factor receptor. J. Cell. Biochem. *20*, 149–161.

Weisz, O. A., and Rodriguez-Boulan, E. (2009). Apical trafficking in epithelial cells: signals, clusters and motors. J. Cell Sci. *122*, 4253–4266.

Wiley, H. S., Herbst, J. J., Walsh, B. J., Lauffenburger, D. A., Rosenfeld, M. G., and Gill, G. N. (1991). The role of kinase activity in endocytosis, compartmentalization, and down-regulation of the epidermal growth factor receptor. J. Biol. Chem. *266*, 11083–11094.

Wilson, P. D. (2004). A plethora of epidermal growth factor-like proteins in polycystic kidneys. Kidney Int. *65*, 2441–2442.

Wilson, P. D., and Robert, S. K. (2008). Mouse models of polycystic kidney disease. In: Current Topics in Developmental Biology, ed. R. Krauss, San Diego: Academic Press, 311–350.

Wu, H., Rossi, G., and Brennwald, P. (2008). The ghost in the machine: small GTPases as spatial regulators of exocytosis. Trends Cell Biol. *18*, 397–404.

Yamaguchi, T., Wallace, D. P., Magenheimer, B. S., Hempson, S. J., Grantham, J. J., and Calvet, J. P. (2004). Calcium restriction allows cAMP activation of the B-Raf/ERK pathway, switching cells to a cAMP-dependent growth-stimulated phenotype. J. Biol. Chem. *279*, 40419–40430.

Yeaman, C., *et al.* (2004). Protein kinase D regulates basolateral membrane protein exit from trans-Golgi network. Nat. Cell Biol. *6*, 106–112.

Yoder, B. K. (2007). Role of primary cilia in the pathogenesis of polycystic kidney disease. J. Am. Soc. Nephrol. *18*, 1381–1388.

Yoder, B. K., Tousson, A., Millican, L., Wu, J. H., Bugg, C. E., Jr., Schafer, J. A., and Balkovetz, D. F. (2002). Polaris, a protein disrupted in orpk mutant mice, is required for assembly of renal cilium. Am. J. Physiol. Renal Physiol. *282*, F541–F552.

Zeng, F., Singh, A. B., and Harris, R. C. (2009). The role of the EGF family of ligands and receptors in renal development, physiology and pathophysiology. Exp. Cell Res. *315*, 602–610.

Zhou, J. (2009). Polycystins and primary cilia: primers for cell cycle progression. Annu. Rev. Physiol. *71*, 83–113.